

# Dark Matter, Neutrino mass, Cutoff for Cosmic-Ray Neutrino, and Higgs Boson Invisible Decay from a Neutrino Portal Interaction

Wen Yin<sup>1</sup>

*IHEP, Chinese Academy of Sciences, Beijing 100049, China*

## Abstract

We study an effective theory beyond the standard model (SM) where either of two additional gauge singlets, a Majorana fermion and a real scalar, constitute all or some fraction of dark matter. The only additional interaction to the SM is via a dimension-five lepton number preserving operator: a neutrino portal interaction. We point out that this interaction (i) generates the neutrino mass radiatively, (ii) gives a cutoff for the cosmic-ray neutrino, and (iii) induces the testable Higgs boson invisible decay in the future lepton colliders, such as the CEPC, ILC, and CLIC. In particular, there are two correlated phenomena. If the dark matter is detected in XENON1T, XENONnT, LZ, DARWIN, or PandaX in future, the Higgs invisible decay is within the reach of the future lepton colliders. If a high energy cutoff of cosmic-ray neutrino, which may account for the non-detection of GZK neutrinos or Glashow resonance, is generated due to its annihilation with the cosmic background neutrino, the Higgs invisible decay can be searched for in these colliders. Moreover, the scale for one of the neutrino mass is predicted. The UV completion and the fine tuning, as well as the constraints from collider physics, cosmology, and astronomy are discussed.

---

<sup>1</sup>email: yinwen@ihep.ac.cn

# 1 Introduction

The Weakly Interacting Massive Particle (WIMP) is a promising particle candidate of dark matter. However, the WIMPs with mass  $6\text{GeV} - \mathcal{O}(10^2)\text{TeV}$  has been severely constrained by the XENON, LUX and PandaX experiments [1–8]. This situation gives the motivation to investigate on a WIMP with mass smaller than GeVs. In this case, the WIMP should be a singlet of the standard model (SM) gauge group to avoid the LEP constraints [9].

If a gauge singlet dark matter is stabilized by a hidden symmetry, its possible interaction with the SM particles is represented by a portal coupling  $\mathcal{O}_{SM}\mathcal{O}_{DM}$ , where  $\mathcal{O}_{SM}$  ( $\mathcal{O}_{DM}$ ) is a SM gauge singlet operator composed only of the SM fields (only of the hidden fields including the dark matter).

In this paper, we focus on the possibility that all or a fraction of the dark matter couples with the SM particles via a neutrino portal interaction, i.e.  $\mathcal{O}_{SM} = \phi_H \cdot L$ . Here  $L$  is a Weyl spinor for a left-handed lepton,  $\phi_H$  is the Higgs doublet field and the dot denotes the contraction of the SU(2) indices. Neutrino portal dark matters are studied by several groups [10–18]. In this paper, we take an effective field theory approach to the new physics based on the strategy of simplicity, and focus on the dimension-five effective operator,

$$\frac{\phi_H \cdot L\psi\phi}{M}, \quad (1)$$

where  $\psi$  ( $\phi$ ) is a Majorana fermion (a real scalar) carrying a hidden  $Z_2$  charge;  $\frac{1}{M}$  is a dimensionful coupling; the lighter one of  $\psi$  and  $\phi$  is identified as the (part of) dark matter. We assume an approximate lepton number symmetry, which suppresses the other dimension-five operators including the Weinberg operator  $(\phi_H \cdot L)^2$ . Since the interaction of (1) at the broken phase of the electroweak symmetry becomes the one in the SLIM scenario [19–21], the 1-loop radiative neutrino mass [22] is generated. The mass difference of  $\psi$  and  $\phi$  is restricted by the neutrino mass bound from the cosmic microwave background (CMB) and baryon acoustic oscillation (BAO) observations as well as neutrinoless double beta decay experiments [23,24]. Thus, the dark matter is accompanied by another particle of similar weight. The parameter space is also restricted by the conditions for the relic abundance of cold dark matter, effective number of neutrino ( $N_{eff}$ ), big-bang nucleosynthesis (BBN), direct detections, and heavy boson decays. On the other hand, depending on the parameter region this scenario has predictions for  $N_{eff}$ , the direct detection of WIMPs, and the Higgs boson decay.

In the parameter region where  $\psi$  constitutes all of the dark matter with mass around  $\mathcal{O}(10)\text{GeV}$ , the loop-induced scattering cross section, between the dark matter and nucleon, becomes large enough [13, 17] to be tested in the direct detection experiments such as XENON1T, XENONnT, LZ, DARWIN, and PandaX in future [25–27]. We show that in this region, in order to annihilate the dark matter enough,  $M$  is small so that the Higgs invisible decay to  $\psi, \phi$  and (anti)neutrino has decay rate within the reach of the future lepton colliders, such as the Circular Electron Positron Collider (CEPC), International Linear Collider (ILC), Compact Linear Collider (CLIC) [28–31]. Namely, if the  $\psi$ –dark matter is detected in the direct detection experiments, our scenario can be confirmed by the measurement of the Higgs boson invisible decay rate in these colliders.

In the region, where  $\psi$  or  $\phi$  is part of the dark matter, the non-detection of the cosmic-ray neutrino event above PeVs, including the non-detection of GZK neutrinos [32–34] and Glashow resonance [35], in the IceCube neutrino observatory [36, 37] may be explained. This is because the cosmic-ray neutrino may annihilate with a cosmic background neutrino due to the interaction (1) before it arrives at the Earth depending on the distance of the neutrino source and  $M$ . If the mean free path of the neutrino is shorter than the order of the particle horizon size, the interaction (1) is required to be so strong as to induce the testable Higgs invisible decay in the future lepton colliders. Moreover, the neutrino mass scale is predicted, e.g. for a cutoff at several PeVs, the neutrino mass is  $\mathcal{O}(10^{-2})\text{eV} - \mathcal{O}(10^{-1})\text{eV}$ . Since the lower limit of the neutrino mass is set from the mass bound of  $\psi$  and  $\phi$  restricted by the observed  $N_{eff}$ , when the neutrino mass is near its lower limit  $\mathcal{O}(10^{-2})\text{eV}$ , the deviation of  $N_{eff}$  is predicted. Our scenario may also be confirmed in the future CMB and BAO observations [38–40].

An UV completion, based on chiral symmetry breaking like in the QCD, is built, in which the origin of  $Z_2$  symmetry, the solution of the hierarchy problem for the scalar mass, and the absence of the tree-level Weinberg term are explained.

This paper is organized as follows. In Sec.2, we will explain the model and the viable parameter region. In Sec.3, the relations of the Higgs boson decay in the future lepton colliders to the direct detection experiments and the cutoff for the cosmic-ray neutrino will be explained. In Sec.4, the UV completion model will be built. The last section is devoted to discussion and conclusions.

## 2 A simple Effective Theory for WIMP

To simplify the discussion, suppose the additional Lagrangian to that of the SM,  $\mathcal{L}_{SM}$ , has only one generation of neutrino,

$$\delta\mathcal{L} = \bar{\psi}\bar{\sigma}^\mu\partial_\mu\psi + \frac{1}{2}(\partial\phi)^2 - \frac{\phi_H \cdot L\psi\phi}{M} - \frac{M_\psi}{2}\psi\psi + h.c - \frac{m_\phi^2}{2}\phi^2 - V(\phi, \phi_H), \quad (2)$$

where the total Lagrangian is given by  $\mathcal{L} = \mathcal{L}_{SM} + \delta\mathcal{L}$ ;  $M_\psi$  ( $m_\phi$ ) is the mass of  $\psi$  ( $\phi$ );  $V(\phi, \phi_H)$  is the potential of the scalar fields which is supposed to give a vanishing vacuum expectation value (VEV),  $\langle\phi\rangle = 0$ , and additional mass squared,  $\langle\frac{\partial^2 V}{\partial\phi^2}\rangle = 0$ , to  $\phi$ . We will assume a small coupling of the Higgs portal term,  $\lambda_H\phi^2|\phi_H|^2$ , in  $V(\phi, \phi_H)$ , so that it is neglected.<sup>1</sup>

The other dimension-five operators,  $(\phi_H \cdot L)^2$ ,  $F_Y^{\mu\nu}\psi\bar{\sigma}_\mu\sigma_\nu\psi$ ,  $|\phi_H|^2\psi^2$ , and  $\phi^2\psi^2$  are neglected due to the approximate lepton number symmetry under which  $L$  and  $\bar{\psi}$  have 1 while others 0.

The extension to the case with three flavors will be discussed in Sec.5.

### 2.1 Neutrino Mass

At the broken phase, one obtains an interaction

$$\frac{v}{M}\nu\psi\phi, \quad (3)$$

where  $v = 174\text{GeV}$  is the VEV of the Higgs field. This interaction is considered in the SLIM scenario [19–21]. Since the lepton number symmetry is slightly broken by  $\frac{M_\psi}{2}\psi\psi$  in Eq.(2), it was pointed out that the neutrino mass is generated at the 1-loop level:

$$m_\nu = \frac{1}{16\pi^2}\frac{v^2}{M^2}KM_\psi + \mathcal{O}\left(\left(\frac{1}{16\pi^2}\right)^2\right)M_\psi, \quad (4)$$

where  $K \equiv K\left(\frac{m_\phi^2}{M_\psi^2}\right)$  with  $K(x) = 1 - \frac{x}{x-1}\log(x)$  satisfying  $\lim_{x \rightarrow 1} K(x) = 1 - x$ .<sup>2</sup> The neutrino mass scale is constrained from the CMB and BAO observations [23] as

$$m_\nu < 0.2\text{eV}(95\%\text{CL}), \quad (5)$$

while the electron Majorana neutrino mass is constrained by the double beta decay experiment [24]. In the left panel of Fig. 1, the contour plot of Eq.(4) and the

<sup>1</sup>The neutrino portal models with Higgs portal term are studied in [13, 16–18]. In this scenario the scalar mass is smaller than  $\mathcal{O}(\text{GeV})$  and if we assume  $\lambda_H \lesssim \frac{m_\phi^2}{v^2}$ , the effect of this term is negligible.

<sup>2</sup>We have taken the renormalization scale  $\Lambda = M_\psi$ .

constraint of (5) (gray shaded region) are represented in  $m_\phi - M$  plane with  $M_\psi = 12\text{MeV}$ . One can see that the constraint from the neutrino mass restricts  $m_\phi$  to be around  $M_\psi$ , and the smaller the  $M$ , the smaller the difference  $|m_\phi - M_\psi|$  is. This is because (5) is either satisfied with a large enough  $M$ , or with a small enough  $|m_\phi - M_\psi|$  in analogy with the supersymmetric cancellation.

## 2.2 Thermal Relic Abundance of dark matter

The dark matter annihilates through the interaction (3) into neutrinos via t(u)-channel. The tree-level annihilation cross sections are given as,

$$\sigma_{\psi\psi}(s) \simeq \frac{1}{16\pi} \left( \frac{v^2}{M^2} \right)^2 \frac{M_\psi^2}{(m_\phi^2 + M_\psi^2)^2} + \mathcal{O}(s), \quad (6)$$

$$\text{and } \sigma_{\phi\phi}(s) \simeq \frac{1}{2\pi} \left( \frac{v^2}{M^2} \right)^2 \frac{M_\psi^2}{(m_\phi^2 + M_\psi^2)^2} + \mathcal{O}(s),$$

for  $\psi\psi$  and  $\phi\phi$  annihilations, respectively. The  $\mathcal{O}(s)$ -terms are calculated by FeynRules and FormCalc [41,42]. FeynRules and FormCalc are also used to confirm all of the amplitude calculations in this paper. The dark matter abundance is estimated as

$$\Omega_{DM}h^2 = 0.1 \left( \frac{4 \times 10^{-26} \text{cm}^3/\text{s}}{\langle \sigma_{eff} v \rangle} \right) \left( \frac{x_f \sqrt{g_*}}{5g_{*s}} \right), \quad (7)$$

where  $\langle \sigma_{eff} v \rangle$  is the thermal averaged annihilation cross section given in [43], where the coannihilation effect is included;  $g_*(g_{*s})$  is the degree of freedom for the energy (entropy) density of the radiation;  $x_f = \frac{T_f}{m_{DM}}$  is the freeze-out temperature in the unit of  $m_{DM} = \min(m_\phi, M_\psi)$ ;  $h = 0.678$ . The region satisfying  $\Omega_{DM}h^2 \simeq 0.1$  is represented by the orange band in the left panel of Fig.1. In the right panel, the contours of  $\Omega_{DM}h^2$  are shown (orange bands) at the limit  $M_\psi = m_\phi$ . The width of the orange bands denotes the ambiguity of our calculation.<sup>3</sup> The gray regions in both sides denote  $\Omega_{DM} > 1$ .

## 2.3 $N_{eff}$ and BBN

The mass of  $\psi$  or  $\phi$  should be larger than MeVs, otherwise the created neutrinos from the annihilation of them will change  $N_{eff}$  by  $\mathcal{O}(1)$  and/or spoil the BBN [45–48].

---

<sup>3</sup>We have fixed  $g_*$ ,  $g_{*s}$  and  $x_f$  to be the typical value for the parameter range under consideration. The width is obtained by using the largest and smallest  $\frac{x_f \sqrt{g_*}}{\sqrt{g_{*s}}}$  in the parameter range. The abundance calculated here is confirmed by micrOMEGAs 4.3.2 [44].

According to [46],

$$m_\phi > 5\text{MeV}, M_\psi > 7\text{MeV} (|m_\phi - M_\psi| \gtrsim \text{MeVs})$$

$$m_\phi, M_\psi > 9\text{MeV} (m_\phi \simeq M_\psi) \quad (8)$$

is obtained from the bound for  $N_{eff}$  (purple vertical band in the left panel.) [23].

On the other hand, the viable region with

$$m_\phi \text{ or } M_\psi \lesssim 11\text{MeV} \quad (9)$$

has a slightly larger  $N_{eff}$  [46], and may be tested by several future CMB observations such as the PIXIE and CMB-S4 experiments, as well as the BAO observation [38–40](the pink shaded region in the left panel.).

## 2.4 Heavy Boson Decays in Colliders

In colliders, this scenario is constrained via heavy boson decay. In particular, we will focus on the Higgs boson invisible decay

$$H \rightarrow \psi + \phi + \nu (\bar{\nu}). \quad (10)$$

Given the Higgs boson total decay width  $\simeq 4\text{MeV}$ , the decay width and the branching ratio of this process are estimated as

$$\Gamma_{H \rightarrow inv} \simeq \frac{1}{1536\pi^3} \frac{m_H^3}{M^2} \text{ and } Br_{H \rightarrow inv} \simeq 0.02\% \left( \frac{10\text{TeV}}{M} \right)^2, \quad (11)$$

respectively. Here  $m_H$  is the Higgs boson mass and the decay products are approximated to be massless. The LHC gives a constraint,  $Br_{H \rightarrow inv} > 58\%(95\%CL)$  [9].  $W^- \rightarrow l^- + inv$  ( $Z \rightarrow \nu + inv$ ) process has a branching ratio deviated from the SM one by  $6 \times 10^{-6}\% \left( \frac{10\text{TeV}}{M} \right)^2$  ( $9 \times 10^{-6}\% \left( \frac{10\text{TeV}}{M} \right)^2$ ),<sup>4</sup> with the corresponding LEP bound given as 0.1% (0.06%) [9]. One finds that  $M$  can be as small as  $\mathcal{O}(100)\text{GeV}$  to be consistent with the current experiments in the light of heavy boson decays. To be conservative, we consider

$$M \gtrsim 400\text{GeV} \quad (12)$$

---

<sup>4</sup>The processes with virtual  $\phi, \psi$  emission and absorption are also included in the decay width to account for the IR divergence for small  $M_\psi$ , and  $m_\phi$ . The decay widths for the corresponding processes are given by  $\Gamma_{W^- \rightarrow l^- + inv} \simeq \Gamma_{W^- \rightarrow l^- + \bar{\nu}_l}^{tree} \left( 1 - \frac{1}{24\pi^2} \left( \frac{v}{M} \right)^2 \right)$  and  $\Gamma_{Z \rightarrow inv} \simeq \Gamma_{Z \rightarrow \bar{\nu} + \nu}^{tree} \left( 3 - \frac{1}{12\pi^2} \left( \frac{v}{M} \right)^2 \right)$ . Here,  $l$  is the charged lepton that participates in the interaction of (1), and  $\Gamma_{\dots}^{tree}$  is the decay width calculated within the SM at the tree-level.

(The horizontal black band in the right panel of Fig.1.). For a small  $M$ , one should care for the constraint for a heavy field in some UV completion models. The constraint in the model, which will be discussed Sec.4, is represented by a lower bound (31) slightly smaller than (12).

On the other hand, the Higgs invisible decay with

$$M \lesssim 5\text{TeV} \tag{13}$$

can be tested in the future Higgs factories, such as the CEPC, ILC, and CLIC, where  $Br_{H \rightarrow inv}$  is measured up to the precision of  $\mathcal{O}(0.1)\%$  (the purple shaded region in the right panel.).

## 2.5 Astronomical/Cosmological Constraints

We would like to mention some astronomical and cosmological constraints, which are avoided non-trivially. From the energy loss/deleptonization in the core of SN1987A, the interaction  $\frac{h}{1\text{TeV}}\nu\nu\phi^2$  for the electron or muon neutrino is constrained as  $10^{-6} < h < 10^{-2}$  when  $m_\phi = 1\text{MeV} - 100\text{MeV}$  [49]. In our scenario  $h \sim (\frac{v}{M})^2 \frac{1\text{TeV}}{M_\psi} \gtrsim 0.1(\frac{10\text{TeV}}{M})^2 \frac{1\text{GeV}}{M_\psi}$  is large enough and  $\phi$  would be trapped in the core.

The neutrino-neutrino scattering cross section has upper-bounds from the CMB observation [50], but the scattering amplitude introduced by the interaction (3) is represented as the sum of 1-loop  $\psi\phi\psi\phi$  box diagrams, and is small.

## 3 Two Regions of Interest

### 3.1 Direct Detection and Higgs Invisible Decay

Supposing that the lighter one of  $\psi$  and  $\phi$  constitutes all of the dark matter, the parameter region with  $\min(M_\psi, m_\phi) \lesssim 6\text{GeV}$  is not severely constrained from the Xenon1T, LUX, and PandaX experiments [1–8], because the nucleon recoil energy due to the scattering with the dark matter is too small. This safe region is represented to the left of the black dotted line in the right panel of Fig.1. On the other hand, one can see that the region to the right of the black dotted line is colored in purple, and hence the Higgs invisible decay to the right of the line is within the reach of the future lepton colliders.

In fact, as shown in [16,17], the  $\psi$ -nucleon scattering amplitude is represented by

a  $Z$ -boson mediating penguin diagram<sup>5</sup> and is suppressed. The amplitude becomes large enough for  $m_\psi \gtrsim 10\text{GeV}$  to be detected in the XENON1T, XENONnT, LZ, DARWIN, and PandaX [4, 26, 27]. Thus, the region with

$$6\text{GeV} < M_\psi < m_\phi \tag{14}$$

can be either tested or constrained.

It follows that if  $\psi$ -dark matter in this region is detected in the direct detection experiments, the reaction of (10) can be searched for in the future lepton colliders.<sup>6</sup>

The scattering amplitudes between  $\phi$  and nucleon, represented by two penguin diagrams with neutrino and anti-neutrino loops, cancel out, and  $\phi$ -dark matter is not constrained as severe as the  $\psi$  case.

### 3.2 Cutoff of Cosmic-Ray Neutrino

The dark matter may also contain other components: a WIMP with neutrino portal interaction (1) for a neutrino with different flavor (See Sec.5), a superpartner<sup>7</sup>, the inflaton [73–82], etc. Thus, we also investigate on the region with  $\Omega_{DM}h^2 < 0.1$  i.e. the region with small  $M$ . In this region, the annihilation between not only WIMPs but also neutrinos is enhanced.

On the other hand, although more statistics are needed, up to now no cosmic neutrino event above  $\mathcal{O}(1)\text{PeV}$  is detected in the IceCube experiment [36, 37] (the

---

<sup>5</sup>In this region, there is some amount of fine tuning to explain the smallness of the neutrino mass,  $\epsilon \equiv \left(\frac{\delta \log(m_\nu)}{\delta \log(m_\phi)}\right)^{-1} \lesssim 10^{-6} \left(\frac{1\text{GeV}}{m_\phi}\right) \left(\frac{M}{1\text{TeV}}\right)^2$ , where the inequality corresponds to that in (5). Thus, one should estimate the neutrino mass by beyond 1-loop order calculations. In this case, the mass difference should be  $|M_\psi - m_\phi| \sim \frac{1}{16\pi^2} M_\psi \gtrsim 1\text{MeV}$ , where the 1- and 2-loop order effects compensate each other in Eq.(4). This relation may kinematically forbid the inelastic scattering to 3body as  $\psi + \text{Nucleon} \rightarrow \phi + \nu + \text{Nucleon}$  in the direct detections of which the typical recoil energy is keVs for  $\mathcal{O}(\text{GeV}s)$  dark matter. This fine tuning and the smallness of  $m_\phi$  are discussed in Sec.5 and Sec.4, respectively.

<sup>6</sup>As long as the dark matter annihilates mainly through the interaction (3), this prediction should hold even if there are other interactions. In this case, the Higgs invisible decay rate should be enhanced due to a different decay process.

<sup>7</sup>There are several typical lightest superpartners (LSPs) which might be the dominant dark matter, depending on SUSY breaking scenarios: gravitino LSP in gauge mediation [89], bino-like LSP with SUSY breaking in a gauge unified manner, wino-like LSP in anomaly mediation and simple SUSY breaking scenarios based on the anomaly mediation [51–59],  $N = 2$  superpartners in  $N = 2$  partial breaking [60–72], etc.

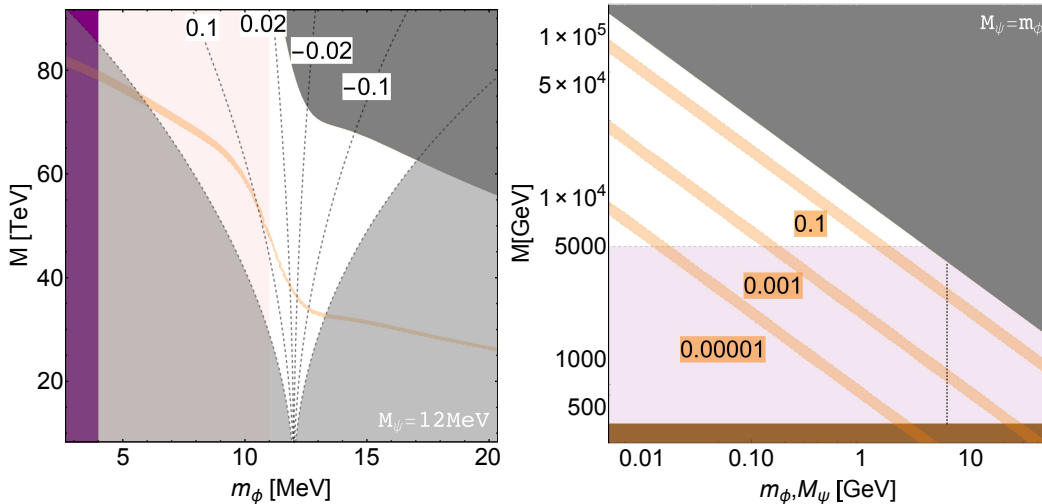


Fig. 1: The contour plots of the neutrino mass with  $M_\psi = 12$  MeV (left) and  $\Omega_{DM}h^2$  with  $M_\psi = m_\phi$  approximation (right). The gray, shaded gray, brown, and purple regions may be excluded by various constraints (See the text). In the left-hand side, the orange band represents  $\Omega_{DM}h^2 \simeq 0.1$  and the shaded pink region may be testable in the future CMB/BAO observations. In the right-hand side, the black dotted line denotes  $M_\psi = m_\phi = 6\text{GeV}$ , and the shaded purple region is testable in the future lepton colliders.

observed neutrino flux is given as the gray points in Fig.3), and the Glashow resonance around 6PeV is also not observed [35]. Despite several detections of cosmic-ray events of other kinds up to  $\sim 10^2\text{EeV}$ , this fact implies that there may be a special cutoff for the cosmic-ray neutrino.

In particular, if some of the observed cosmic-rays around  $10^2\text{EeV}$  are nucleons or light nuclei, cosmic-ray neutrinos can be produced. The proton of energy larger than  $\mathcal{O}(10^2)\text{EeV}$  interacts with the CMB-photon and produces pions via  $\Delta$ -resonance, and hence loses energy before it reaches the Earth. This scattering sets a GZK cutoff at energy  $\mathcal{O}(10^2)\text{EeV}$  for protons [83,84] which may explain the observed cutoff for high energy cosmic-ray events. Thus, GZK neutrinos of energy  $\mathcal{O}(\text{EeV})$  are generated via the decay of these pions [85], and should be detected at  $\mathcal{O}(0.1) - \mathcal{O}(10)$  events/year in the IceCube neutrino observatory [32–34].

The non-detection of energetic neutrino events may be explained from a viewpoint of particle physics.<sup>8</sup> In this scenario, the annihilation between the cosmic-ray and

<sup>8</sup>There are also astronomical explanations for the absence of neutrino events above several PeVs.

the cosmic background neutrinos,

$$\nu/\bar{\nu} + \nu(C\nu B) \rightarrow \psi + \psi, \phi + \phi, \quad (15)$$

can be enhanced with a small  $M$ , so that before the neutrinos reach the Earth the reaction takes place. Namely, the existence of  $\psi$  and  $\phi$  as well as the interaction of (3) can set a ‘‘GZK cutoff’’ for neutrinos.

This cutoff is represented by two conditions. First, the non-detection of the neutrino event for  $E_\nu > E_\nu^{cutoff}$  implies that the center of mass energy of the neutrino-(anti)neutrino system,  $E_{cm}$ , becomes greater than the threshold,  $2M_\psi$  or  $2m_\phi$ , at  $E_\nu^{cutoff}$  so that the annihilation-channel is turned on at

$$\frac{E_{cm}}{2} \equiv \frac{1}{\sqrt{2}} \sqrt{m_\nu^2 + E_\nu E_{C\nu B} (1 - \cos \theta)} \gtrsim \left( \frac{E_\nu^{cutoff}}{6\text{PeV}} \frac{E_{C\nu B}}{0.2\text{eV}} \right)^{\frac{1}{2}} 35\text{MeV} \sim M_\psi \text{ or } m_\phi. \quad (16)$$

Here,  $E_{C\nu B} \simeq \max[T_\nu, m_\nu]$  is the typical energy of cosmic background neutrinos with temperature  $T_\nu \simeq 2 \times 10^{-4}\text{eV}$ , and  $\theta$  is the angle between the momenta of two neutrinos.

Secondly, the annihilation cross section for the process (15) should be large to give a neutrino mean free path,  $d(E_\nu)$ , short enough. To discuss this, let us assume for simplicity that there is only one kind of neutrino, and it has the interaction (1).<sup>9</sup>

By following [88], one obtains the mean free path of a neutrino as

$$d(E_\nu) \simeq \int \frac{d^3\vec{p}}{(2\pi)^3} \sigma_{\nu\nu}(E_{cm}(\vec{p}, E_\nu)) f_{C\nu B}(\vec{p}). \quad (17)$$

Here,  $\sigma_{\nu\nu}(E_{cm})$  is the helicity averaged neutrino-(anti)neutrino annihilation cross section, and  $f_{C\nu B}(\vec{p}) = 2(e^{|\vec{p}|/T_\nu} + 1)^{-1}$  is the neutrino distribution function for the cosmic background neutrinos.

Since the neutrino mass constraint (5) requires  $m_\phi \simeq M_\psi$  from Eq.(4) and a small

---

For example, if the neutrino is originated from the galaxy clusters or starburst galaxies the non-observation of the Glashow resonance can be accounted for [86]. If the  $\mathcal{O}(10^2)\text{EeV}$  cosmic-rays observed are composed of heavy nuclei such as iron, the absence of the GZK neutrino event can be explained [87].

<sup>9</sup>Given the neutrino oscillation, all kinds of the neutrinos share the interaction of (1) and the mean free path for each neutrino should be Eq.(17) times a factor  $\sim \mathcal{O}(1)$ . Thus, in the multi-flavor extension of the interaction (1), one does not need all the interactions to be strong to set the cutoff for different kinds of neutrinos.

$M$ , we assume  $M_\psi = m_\phi$  to simplify the following discussion, e.g.

$$\sigma_{\nu\nu} \simeq \frac{v^4 \sqrt{\left(\frac{E_{cm}}{2}\right)^2 - m_\phi^2} + E_{cm} \log\left(\frac{\sqrt{\left(\frac{E_{cm}}{2}\right)^2 - m_\phi^2} + \frac{E_{cm}}{2}}{m_\phi}\right)}{M^4 32\pi^2 E_{cm}^3}. \quad (18)$$

Then, the neutrino flux from the source at the  $L$  distant place is weakened by a factor of

$$\kappa(E_\nu) = e^{-\frac{L}{d(E_\nu)}}. \quad (19)$$

Here, we have neglected the effect of the redshift for  $E_\nu$  due to the expansion of the Universe, which would reduce the observed  $E_\nu$  in the IceCube by  $\mathcal{O}(10)\%$  with  $L \sim \mathcal{O}(1)\text{Gpc}$ .

The contour plot of  $d(E_\nu)$  is represented in Fig.2. From the left panel, one finds that the neutrino flux originating from a place with

$$L > \mathcal{O}(10)\text{Mpc} \quad (20)$$

can be affected by our scenario.

As a demonstration, the predicted neutrino flux is represented in Fig.3 by assuming the neutrino flux distribution at  $M \rightarrow \infty$  limit to be

$$\Phi(E_\nu)E_\nu^2 = 1.5 \times 10^{-8} \left(\frac{E_\nu}{10^5\text{GeV}}\right)^{-0.3} + V_{GZK}(E_\nu) \quad (21)$$

(the gray solid line in Fig.3). The first term is the best-fit power law in [37] while the second term represents a hill for a simplified GZK neutrino flux as a demonstration,  $10^8 V_{GZK}(E_\nu) = \left(e^{\left(\frac{3}{8} \cos\left(\pi \frac{\log_{10}(E_\nu/\text{GeV}) - 8.75}{2.5}\right) - \frac{1}{24} \cos\left(3\pi \frac{\log_{10}(E_\nu/\text{GeV}) - 8.75}{2.5}\right)\right)} - e^{-\frac{1}{3}}\right)$  for  $E_\nu > 10^{6.25}\text{GeV}$ , otherwise 0. (For realistic ones of GZK neutrino flux, see [32–34].) The neutrino flux in our scenario is roughly estimated as

$$\kappa(E_\nu)\Phi(E_\nu)E_\nu^2. \quad (22)$$

In Fig.3, unlike the absorption lines obtained in [88], the neutrino flux does get a cutoff (or an absorption band depending on the original neutrino flux). This is because the annihilation (15) is in t/u-channel with much weaker  $E_\nu$  dependence than the s-channel ones.

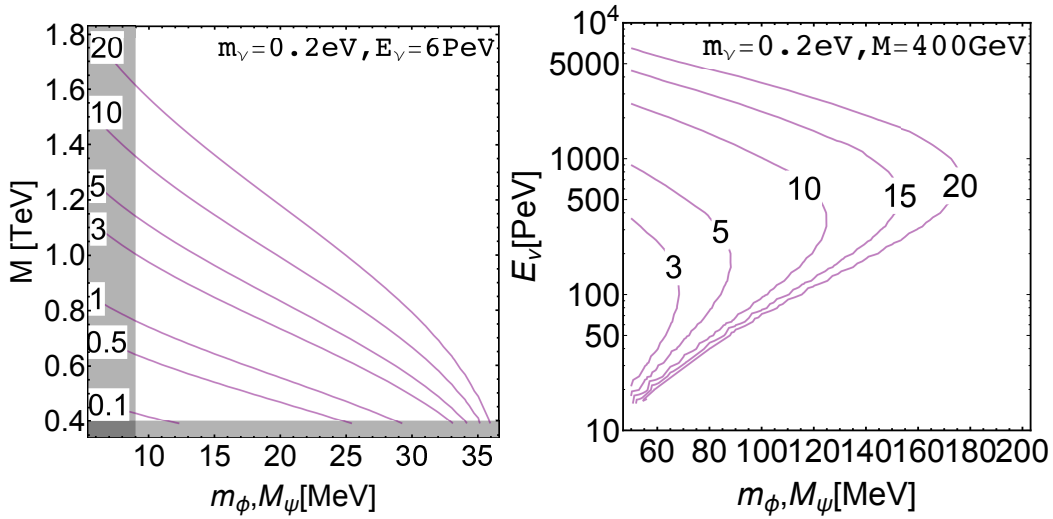


Fig. 2: The contour plot of the mean free path  $d(E_\nu)$  [Gpc] for neutrino with  $m_\nu = 0.2\text{eV}$  and  $M_\psi = m_\phi$  approximation. In the left panel,  $E_\nu = 6\text{PeV}$  is fixed. The horizontal (vertical) shaded region represents the constrained region for SM Heavy boson decay (neutrino effective number). In the right panel  $M = 400\text{GeV}$  is fixed.

### Parameter Range and Higgs Boson Decay

As in the left panel of Fig. 2, we have checked that to obtain a  $d(E_\nu)$  smaller than the scale of particle horizon size  $\sim \mathcal{O}(10)\text{Gpc}$ ,  $M$  should be smaller than  $2\text{TeV}$ . From the right panel of Fig. 2, since  $M$  is at its lower bound (12), one reads the upper bound of  $M_\psi \simeq m_\phi$  as  $M_\psi \simeq m_\phi < 150\text{MeV}$ . Hence one obtains the parameter range that can affect the neutrino flux through the detector of the IceCube,

$$M \simeq 0.4 - 2\text{TeV} \text{ and } m_\phi \simeq M_\psi \sim 9 - 150\text{MeV}. \quad (23)$$

Since the upper bound of  $M$  satisfies (13) and the upper bound of  $m_\phi + M_\psi$  is smaller than the Higgs boson mass, the following is predicted: if the high energy neutrino flux in the IceCube is affected in this scenario, the Higgs invisible decay, with branching ratio Eq.(11), is within the reach of the CEPC, ILC, and CLIC.

### Prediction of Neutrino Mass Range

The left panel of Fig.2 illustrates that given  $E_\nu = 6\text{PeV}$ ,  $d(E_\nu)$  increases rapidly when  $m_\phi \simeq M_\psi$  approaches to  $35\text{MeV}$ . The increasing point corresponds to the cutoff at  $E_\nu^{cutoff} \simeq 6\text{PeV}$ , since the process (15) is forbidden from the inequality in (16) for a larger mass. The same cutoff can also be obtained from a smaller  $m_\phi \simeq M_\psi$ , if

the neutrino mass is smaller. Since there is a lower bound (8) for  $M_\psi \simeq m_\phi$ , with given  $E_\nu^{cutoff}$  the neutrino mass acquires a lower bound, e.g.  $m_\nu \gtrsim 1.4 \times 10^{-2} \text{eV}$  for a cutoff at 6PeV. From Eq.(16), one expects that the smaller the cutoff, the larger the lower bound of  $m_\nu$ . Namely, if there is a cutoff at  $\lesssim 6\text{PeV}$ , which may explain the non-observation of the Glashow resonance, the neutrino mass range is predicted to be

$$m_\nu \simeq 0.01 - 0.2\text{eV} \text{ (for } E_\nu^{cutoff} \lesssim 6\text{PeV}). \quad (24)$$

The neutrino flux around the lower limit is illustrated by the purple dotted line in Fig.3. Interestingly, the predicted neutrino mass range, to provide a cutoff below the scale of the Glashow resonance, is around the atmospheric (solar) neutrino scale 0.05eV (0.009eV).

Since near the lower bound of  $m_\nu$  for a given cutoff energy,  $M_\psi \simeq m_\phi$  is around its lower bound 9MeV, the neutrinos produced via the annihilation of  $\psi$  and  $\phi$  in the early Universe contribute to a slight deviation of  $N_{eff}$ . The deviation may be confirmed by the future CMB and BAO observations. For example, for  $E_\nu^{cutoff} \simeq 6\text{PeV}$ , in the range of  $0.01\text{eV} \lesssim m_\nu \lesssim 0.02\text{eV}$ , correspondingly  $9\text{MeV} \lesssim M_\psi \simeq m_\phi \lesssim 11\text{MeV}$ , the deviation of  $N_{eff}$  may be tested.

If there is a cutoff around 1EeV, which may explain the non-detection of the GZK neutrinos, the neutrino mass range can be estimated from Eq.(16) and the mass range of  $9\text{MeV} < m_\phi \simeq M_\psi \lesssim 100\text{MeV}$  (the right-hand side can be read from the left panel of Fig.2) as

$$m_\nu \simeq 0.00008 - 0.01\text{eV} (E_\nu^{cutoff} = 1\text{EeV}). \quad (25)$$

The flux with a cutoff around EeV is represented by the blue dashed line in Fig.3. Since the upper bound of  $m_\nu$  is set by the too long mean free path, this upper bound decreases if the lower bound of  $M$  increases due to some experiments.

## 4 UV Completion and Naturalness for $m_\phi$

The higher dimensional term (1) implies a new physics appears around the scale  $M$ . A simple UV completion, that generates the term (1) and preserves lepton number, is

$$\mathcal{L} = -y\phi_H LN - \tilde{M}SN - \frac{\tilde{M}}{2f}\phi S\psi \quad (26)$$

where  $S$  and  $N$  are heavy gauge singlet Dirac fermions with lepton number 1 and -1, respectively. For later convenience, we introduce a Yukawa coupling  $y$ , the decay

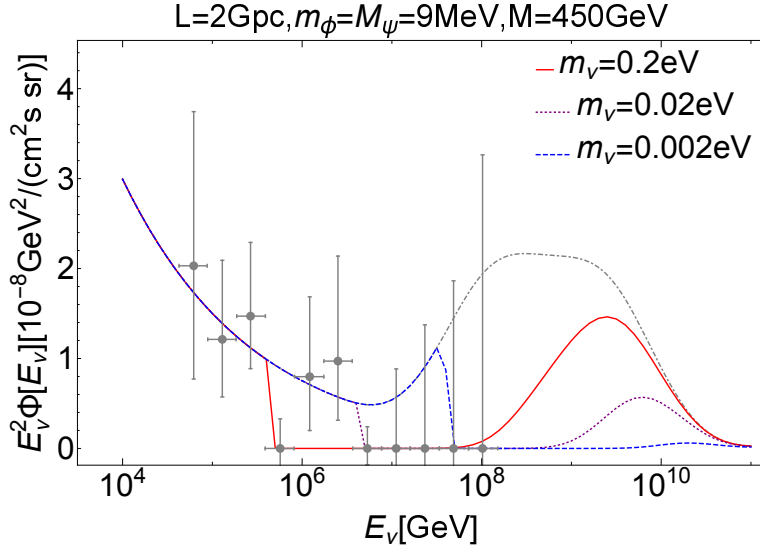


Fig. 3: The predicted neutrino flux with several  $m_\nu$ .  $L = 2\text{Gpc}$ ,  $M_\psi = m_\phi = 9\text{MeV}$  and  $M = 450\text{GeV}$  are fixed. The red solid, purple dotted, and blue dashed lines represent the flux with  $m_\nu$  taking  $0.2\text{eV}$ ,  $0.02\text{eV}$ , and  $0.002\text{eV}$ , respectively. The gray points represent the IceCube observation arranged from [37] while the gray dot-dashed line represents Eq.(21).

constant  $f$  for  $\phi$  and the Dirac mass  $\tilde{M}$  for  $S$  and  $N$ . By integrating out  $S$  and  $N$  at the tree-level, the term (1) is generated with

$$\frac{1}{M} = -\frac{y}{2f}. \quad (27)$$

Since  $y$  is constrained [90], if  $M$  is small,  $f$  should be small.

On the other hand, the existence of a light scalar  $\phi$  suggests a naturalness problem. One of the solutions to this problem<sup>10</sup> is to identify  $\phi$  as a pseudo-Nambu-Goldstone boson, where the  $Z_2$  symmetry is part of the residual symmetry. Now consider the spontaneously breaking of an approximate  $SU(2) \times U(1)$  global symmetry to  $U(1)$  by some non-perturbative effect in analogy with the chiral symmetry breaking in QCD. If all the explicit breaking terms of  $SU(2) \times U(1)$  have even charges under the residual  $U(1)$ , this residual symmetry contains an exact  $Z_2$  symmetry. The

<sup>10</sup>Alternatively, this may indicate that a SUSY extension of the SM has a SUSY breaking soft scale around MeVs in the  $Z_2$  odd sector, while that in the SM sector is above TeV to survive the experimental constraints. A candidate is the gauge mediation scenario [89], where the sparticles charged under the SM gauge gain weight via gauge interaction, while a singlet scalar acquires a highly suppressed mass either from higher order correction or the gravity effects.

U(1) charged pion, say  $\pi_+$ , is  $Z_2$  odd and contains  $\phi$  as  $\pi_+ = \frac{\phi+i\tilde{\phi}}{\sqrt{2}}$ . This possibility not only explains the smallness of  $m_\phi$ , but also allows a rather small decay constant,  $f$ , for the composite scalar  $\phi$ , like the pion decay constant in QCD.

To be concrete, let us consider the following non-linear realized Lagrangian for pions,

$$\mathcal{L}_{UV} = \mathcal{L}_{sym} + \mathcal{L}_{exb} \quad (28)$$

$$\mathcal{L}_{sym} = \bar{\vec{N}} \vec{\sigma}^\mu \partial_\mu \vec{N} - \langle \vec{\Phi} \rangle \cdot e^{i \frac{\pi^a \sigma_a}{2f}} \cdot \vec{N} S + h.c., \quad (29)$$

$$\mathcal{L}_{exb} = -\frac{M_\psi}{2} \psi \psi - M_N N N - \frac{m_\phi^2}{2} \phi^2 - \frac{\tilde{m}^2}{2} \tilde{\phi}^2 - \frac{m_0^2}{2} \pi_0^2 - y \phi_H \cdot L N + h.c. \quad (30)$$

Here,  $\mathcal{L}_{sym}$  is  $SU(2) \times U(1)$  symmetric Lagrangian, while terms, which explicitly break  $SU(2) \times U(1)$ , are collected in  $\mathcal{L}_{exb}$ ;  $\vec{N} = (N, \psi)$  is a matter doublet with U(1) charge  $-1/2$  and lepton number  $-1$ , while the fermion  $S$  carries a lepton number  $1$ ;  $\langle \vec{\Phi} \rangle = (\tilde{M}, 0)$  is the VEV of an  $SU(2)$  doublet operator with U(1) charge  $-1/2$ , and the second term of Eq.(29) turns out to be the second and third terms in Eq.(26).

The mass parameters of  $M_\psi, m_\phi, \tilde{m}, m_0$  and  $M_N$ , which are the explicit breaking terms of the  $SU(2) \times U(1)$  symmetry, can be much smaller than  $\tilde{M}$  and  $f$  naturally. In addition, we have assumed that  $S$  and  $\Phi$  are charged oppositely under an approximate symmetry so that the Majorana mass term of  $S$  is neglected in Eq.(30). Notice two facts. First, due to the absence of the Majorana mass term of  $S$ , no Weinberg term is generated after diagonalizing the mass matrix for the leptons. Secondly, in Eq.(30) the unbroken U(1) is explicitly broken down to exact  $Z_2$  symmetry by  $M_\psi$  and  $\tilde{m}^2 - m_\phi^2$ .

This effective theory should have a cutoff scale smaller than  $\sim 4\pi f$  as in the QCD case, which turns to be a consistency condition,  $|\tilde{M}| < 4\pi f$ . If we adapt the constraint in [90] for a heavy right-handed neutrino, which dominantly mixes with  $\tau$  neutrino,  $\left| \frac{y\psi}{M} \right| \lesssim 0.1$  is required. Thus, one obtains

$$M \gtrsim \frac{v}{0.1 \times 2\pi} \sim 300 \text{ GeV}. \quad (31)$$

The parameter region analyzed in the previous sections can be identified as the subregion of this model with  $\pi_0$  and  $\tilde{\phi}$  decoupled.

Since the first term in Eq.(26) explicitly breaks the  $SU(2) \times U(1)$  symmetry at a perturbative level,  $\phi$  in  $\pi_+$  gets mass from radiative corrections. Due to the exact  $Z_2$  symmetry, the explicit  $SU(2) \times U(1)$  breaking term is  $\simeq \frac{y\phi^2}{8f^2} \phi_H \cdot L N$  in the mass basis of  $N$  and  $S$ . The radiative corrections to  $m_\phi^2$  are suppressed at the

2-loop level as,  $\delta m_\phi^2 \sim \left(\frac{1}{16\pi^2}\right)^2 \frac{y^2 \tilde{M}^4}{4f^2} \sim \left(\left(\frac{\tilde{M}}{125\text{GeV}}\right)^2 \left(\frac{1\text{TeV}}{M}\right)\right)^2 (90\text{MeV})^2$ , while the radiative corrections to the Higgs portal term,  $\frac{\lambda_p}{2} |H|^2 \phi^2$ , are at the 1-loop level as  $\delta\lambda_p \sim (1\text{GeV})^2 \frac{1}{v^2} \left(\frac{\tilde{M}}{125\text{GeV}} \frac{1\text{TeV}}{M}\right)^2$ . The region with  $7\text{GeV} \lesssim \tilde{M} < 125\text{GeV}$  is excluded due to the constraint of the Higgs invisible decay to  $N$  and  $\nu_\tau$  in the LHC. In the region with  $\tilde{M} \lesssim 7\text{GeV}$ , not only the radiative corrections are suppressed, but also the Higgs boson invisible decay may be tested in the future lepton colliders.

## 5 Discussion and Conclusions

Realistically, to explain the neutrino oscillation one should make an extension of the interaction (1) to that with more generations: e.g.  $\phi_H \cdot L^i Y_{ij} M^{-1} \psi^j \phi$ , ( $\phi_H \cdot L^i Y_{ij} M^{-1} \psi^j \phi^j$ ) where  $i, j$  denotes the generation and  $Y_{ij}$  is the dimensionless coupling in the mass basis of  $\psi^j$  ( $\phi^j$ ). The neutrino mass matrix is generated as  $m_{\nu ij} \simeq \frac{\sum_k Y_{ik} M_{\psi k} Y_{kj} K_k v^2}{16\pi^2 M^2} \left( \frac{\sum_k Y_{ik} Y_{kj} K_k M_\psi v^2}{16\pi^2 M^2} \right)$  where  $K_j$  is  $K$  in Eq.(4) but with  $M_\psi$  ( $m_\phi$ ) replaced by the mass of  $\psi_j$  ( $\phi_j$ ). In this extension, several parameter regions previously discussed can be simultaneously realized by the neutrino portal interactions of different flavors.

In Sec.4 the naturalness of  $m_\phi$  was discussed while there is still a fine tuning between  $m_\phi$  and  $M_\psi$  to explain the neutrino mass (4). This tuning may be anthropically explained [91–94]. Alternatively, this tuning can be alleviated by replacing the real scalar field with a complex one,  $\pi_+$  as in Sec.4. As discussed in [19–21], if the U(1) breaking parameter  $\tilde{\epsilon}$  in  $m_\phi^2 - m_{\tilde{\phi}}^2 \equiv \tilde{\epsilon} m_\phi^2$  is small, the neutrino mass (4) is suppressed by an additional factor of  $\tilde{\epsilon}$ . The prediction in Sec.3.1 and Sec.3.2 would not change much. This is because for a given values of  $\min(M_\psi, m_{\tilde{\phi}}, m_\phi)$  and the cross section for dark matter-dark matter or neutrino-(anti)neutrino annihilation, the increase of  $\max(m_{\tilde{\phi}}, m_\phi, M_\psi)$  leads to the decrease of  $M$ . Thus, the Higgs invisible decay rate is even enhanced, while the predicted neutrino mass range is slightly enlarged due to the relaxed constraint of (8).

In this paper, an effective theory for WIMPs charged under a hidden symmetry was investigated, where the WIMPs only have a dimension-5 neutrino portal coupling that plays the role in the interaction with the SM particles. In particular, we had two rigid predictions based on two situations. First, if one of the WIMPs here is detected as the dark matter in XENON1T, XENONnT, LZ, or DARWIN, the Higgs boson invisible decay can be searched for in the CEPC, ILC and CLIC. Secondly, if

the cosmic-ray neutrino obtains a cutoff at a given energy due to this interaction, the Higgs invisible decay is searched for in these colliders. Moreover, the range of the neutrino mass is predicted from the mass range of the WIMPs.

A UV completion model based on chiral symmetry breaking was introduced to explain the naturalness for the light singlet scalar, and the strong coupling of the higher dimensional term which is needed in the interesting parameter regions. The real singlet scalar in the neutrino portal interaction is identified as a pseudo-Nambu-Goldston boson. The hidden symmetry is explained as the residual symmetry. The absence of the Weinberg operator at the tree-level is also explained.

## Acknowledgement

I would like to thank Adam Falkowski, Fapeng Huang, and Hao Zhang for collaboration at an early stage of this work. I also thank Hiroyuki Ishida and Yingnan Mao for useful discussions, and thank Hiromasa Takaura for carefully reading the manuscript.

## References

- [1] D. S. Akerib *et al.* [LUX Collaboration], Phys. Rev. Lett. **112** (2014) 091303 [arXiv:1310.8214 [astro-ph.CO]].
- [2] M. Xiao *et al.* [PandaX Collaboration], Sci. China Phys. Mech. Astron. **57**, 2024 (2014) [arXiv:1408.5114 [hep-ex]].
- [3] D. S. Akerib *et al.* [LUX Collaboration], Phys. Rev. Lett. **116**, no. 16, 161301 (2016) [arXiv:1512.03506 [astro-ph.CO]].
- [4] D. S. Akerib *et al.* [LUX Collaboration], Phys. Rev. Lett. **118**, no. 2, 021303 (2017) [arXiv:1608.07648 [astro-ph.CO]].
- [5] A. Tan *et al.* [PandaX Collaboration], Phys. Rev. D **93**, no. 12, 122009 (2016) [arXiv:1602.06563 [hep-ex]].
- [6] E. Aprile *et al.* [XENON100 Collaboration], Phys. Rev. D **94**, no. 12, 122001 (2016) [arXiv:1609.06154 [astro-ph.CO]].
- [7] C. Fu *et al.* [PandaX-II Collaboration], Phys. Rev. Lett. **118**, no. 7, 071301 (2017) [arXiv:1611.06553 [hep-ex]].

- [8] E. Aprile *et al.* [XENON Collaboration], arXiv:1705.06655 [astro-ph.CO].
- [9] C. Patrignani *et al.* [Particle Data Group], Chin. Phys. C **40**, no. 10, 100001 (2016).
- [10] D. E. Kaplan, M. A. Luty and K. M. Zurek, Phys. Rev. D **79**, 115016 (2009) [arXiv:0901.4117 [hep-ph]].
- [11] A. Falkowski, J. Juknevich and J. Shelton, arXiv:0908.1790 [hep-ph].
- [12] A. Falkowski, J. T. Ruderman and T. Volansky, JHEP **1105**, 106 (2011) [arXiv:1101.4936 [hep-ph]].
- [13] M. Escudero, N. Rius and V. Sanz, arXiv:1607.02373 [hep-ph].
- [14] B. Bertoni, S. Ipek, D. McKeen and A. E. Nelson, JHEP **1504**, 170 (2015) [arXiv:1412.3113 [hep-ph]].
- [15] J. F. Cherry, A. Friedland and I. M. Shoemaker, arXiv:1411.1071 [hep-ph].
- [16] V. Gonzalez Macias and J. Wudka, JHEP **1507**, 161 (2015) [arXiv:1506.03825 [hep-ph]].
- [17] V. Gonzalez-Macias, J. I. Illana and J. Wudka, JHEP **1605**, 171 (2016) [arXiv:1601.05051 [hep-ph]].
- [18] B. Batell, T. Han and B. S. E. Haghi, arXiv:1704.08708 [hep-ph].
- [19] C. Boehm, Y. Farzan, T. Hambye, S. Palomares-Ruiz and S. Pascoli, Phys. Rev. D **77**, 043516 (2008) [hep-ph/0612228].
- [20] Y. Farzan, Phys. Rev. D **80**, 073009 (2009) [arXiv:0908.3729 [hep-ph]].
- [21] Y. Farzan, Int. J. Mod. Phys. A **26**, 2461 (2011) [arXiv:1106.2948 [hep-ph]].
- [22] E. Ma, Phys. Rev. D **73**, 077301 (2006) [hep-ph/0601225].
- [23] P. A. R. Ade *et al.* [Planck Collaboration], Astron. Astrophys. **594**, A13 (2016) [arXiv:1502.01589 [astro-ph.CO]].
- [24] A. Gando *et al.* [KamLAND-Zen Collaboration], Phys. Rev. Lett. **117**, no. 8, 082503 (2016) Addendum: [Phys. Rev. Lett. **117**, no. 10, 109903 (2016)] [arXiv:1605.02889 [hep-ex]].
- [25] E. Aprile *et al.* [XENON Collaboration], JCAP **1604**, no. 04, 027 (2016) [arXiv:1512.07501 [physics.ins-det]].
- [26] D. S. Akerib *et al.* [LZ Collaboration], arXiv:1509.02910 [physics.ins-det].

- [27] J. Aalbers *et al.* [DARWIN Collaboration], JCAP **1611**, 017 (2016) [arXiv:1606.07001 [astro-ph.IM]].
- [28] CEPC-SPPC Study Group,  
[http://cepc.ihep.ac.cn/preCDR/main\\_preCDR.pdf](http://cepc.ihep.ac.cn/preCDR/main_preCDR.pdf)
- [29] CEPC-SPPC Study Group,  
[http://cepc.ihep.ac.cn/preCDR/Pre-CDR\\_final\\_20150317.pdf](http://cepc.ihep.ac.cn/preCDR/Pre-CDR_final_20150317.pdf)
- [30] D. M. Asner *et al.*, arXiv:1310.0763 [hep-ph].
- [31] H. Abramowicz *et al.*, arXiv:1608.07538 [hep-ex].
- [32] M. Ahlers, L. A. Anchordoqui, M. C. Gonzalez-Garcia, F. Halzen and S. Sarkar, Astropart. Phys. **34**, 106 (2010) [arXiv:1005.2620 [astro-ph.HE]].
- [33] G. B. Gelmini, O. Kalashev and D. V. Semikoz, JCAP **1201**, 044 (2012) [arXiv:1107.1672 [astro-ph.CO]].
- [34] R. Y. Liu, A. M. Taylor, X. Y. Wang and F. A. Aharonian, Phys. Rev. D **94**, no. 4, 043008 (2016) [arXiv:1603.03223 [astro-ph.HE]].
- [35] S. L. Glashow, Phys. Rev. **118**, 316 (1960).
- [36] M. G. Aartsen *et al.* [IceCube Collaboration], Science **342**, 1242856 (2013) [arXiv:1311.5238 [astro-ph.HE]].
- [37] M. G. Aartsen *et al.* [IceCube Collaboration], Phys. Rev. Lett. **113**, 101101 (2014) [arXiv:1405.5303 [astro-ph.HE]].
- [38] A. Kogut *et al.*, JCAP **1107**, 025 (2011) [arXiv:1105.2044 [astro-ph.CO]].
- [39] K. N. Abazajian *et al.* [CMB-S4 Collaboration], arXiv:1610.02743 [astro-ph.CO].
- [40] D. Baumann, D. Green and M. Zaldarriaga, arXiv:1703.00894 [astro-ph.CO].
- [41] T. Hahn and M. Perez-Victoria, Comput. Phys. Commun. **118**, 153 (1999) [hep-ph/9807565].
- [42] A. Alloul, N. D. Christensen, C. Degrande, C. Duhr and B. Fuks, Comput. Phys. Commun. **185**, 2250 (2014) [arXiv:1310.1921 [hep-ph]].
- [43] G. Belanger, F. Boudjema, A. Pukhov and A. Semenov, Comput. Phys. Commun. **149**, 103 (2002) [hep-ph/0112278].
- [44] D. Barducci, G. Belanger, J. Bernon, F. Boudjema, J. Da Silva, S. Kraml, U. Laa and A. Pukhov, arXiv:1606.03834 [hep-ph].

- [45] C. Boehm, M. J. Dolan and C. McCabe, JCAP **1308**, 041 (2013) [arXiv:1303.6270 [hep-ph]].
- [46] K. M. Nollett and G. Steigman, Phys. Rev. D **91** (2015) no.8, 083505 [arXiv:1411.6005 [astro-ph.CO]].
- [47] P. D. Serpico and G. G. Raffelt, Phys. Rev. D **70**, 043526 (2004) [astro-ph/0403417].
- [48] E. W. Kolb, M. S. Turner and T. P. Walker, Phys. Rev. D **34**, 2197 (1986).
- [49] L. Heurtier and Y. Zhang, JCAP **1702**, no. 02, 042 (2017) [arXiv:1609.05882 [hep-ph]].
- [50] F. Y. Cyr-Racine and K. Sigurdson, Phys. Rev. D **90**, no. 12, 123533 (2014) [arXiv:1306.1536 [astro-ph.CO]].
- [51] L. Randall and R. Sundrum, Nucl. Phys. B **557**, 79 (1999) [hep-th/9810155].
- [52] G. F. Giudice, M. A. Luty, H. Murayama and R. Rattazzi, JHEP **9812**, 027 (1998) [hep-ph/9810442].
- [53] A. Pomarol and R. Rattazzi, JHEP **9905**, 013 (1999) [hep-ph/9903448].
- [54] Z. Chacko, M. A. Luty, I. Maksymyk and E. Ponton, JHEP **0004**, 001 (2000) [hep-ph/9905390].
- [55] M. Ibe, T. Moroi and T. T. Yanagida, Phys. Lett. B **644**, 355 (2007) [hep-ph/0610277].
- [56] M. Ibe and T. T. Yanagida, Phys. Lett. B **709**, 374 (2012) [arXiv:1112.2462 [hep-ph]].
- [57] N. Arkani-Hamed, A. Gupta, D. E. Kaplan, N. Weiner and T. Zorawski, arXiv:1212.6971 [hep-ph].
- [58] W. Yin and N. Yokozaki, Phys. Lett. B **762**, 72 (2016) [arXiv:1607.05705 [hep-ph]].
- [59] T. T. Yanagida, W. Yin and N. Yokozaki, JHEP **1609**, 086 (2016) [arXiv:1608.06618 [hep-ph]].
- [60] M. M. Nojiri and M. Takeuchi, Phys. Rev. D **76**, 015009 (2007) [hep-ph/0701190].
- [61] G. Belanger, K. Benakli, M. Goodsell, C. Moura and A. Pukhov, JCAP **0908**, 027 (2009) [arXiv:0905.1043 [hep-ph]].

- [62] N. Polonsky and S. f. Su, Phys. Rev. D **63**, 035007 (2001) [hep-ph/0006174].
- [63] K. Benakli and M. D. Goodsell, Nucl. Phys. B **830**, 315 (2010) [arXiv:0909.0017 [hep-ph]].
- [64] E. J. Chun, J. C. Park and S. Scopel, JCAP **1002**, 015 (2010) [arXiv:0911.5273 [hep-ph]].
- [65] A. De Simone, V. Sanz and H. P. Sato, Phys. Rev. Lett. **105**, 121802 (2010) [arXiv:1004.1567 [hep-ph]].
- [66] M. Heikinheimo, M. Kellerstein and V. Sanz, JHEP **1204**, 043 (2012) [arXiv:1111.4322 [hep-ph]].
- [67] K. Benakli, M. D. Goodsell and F. Staub, JHEP **1306**, 073 (2013) [arXiv:1211.0552 [hep-ph]].
- [68] E. Dudas, M. Goodsell, L. Heurtier and P. Tziveloglou, Nucl. Phys. B **884**, 632 (2014) [arXiv:1312.2011 [hep-ph]].
- [69] K. Benakli, M. Goodsell, F. Staub and W. Porod, Phys. Rev. D **90**, no. 4, 045017 (2014) [arXiv:1403.5122 [hep-ph]].
- [70] M. D. Goodsell, M. E. Krauss, T. Muller, W. Porod and F. Staub, JHEP **1510**, 132 (2015) [arXiv:1507.01010 [hep-ph]].
- [71] Y. Shimizu and W. Yin, Phys. Lett. B **754**, 118 (2016) [arXiv:1509.04933 [hep-ph]].
- [72] W. Yin, arXiv:1609.03527 [hep-ph].
- [73] L. Kofman, A. D. Linde and A. A. Starobinsky, Phys. Rev. Lett. **73**, 3195 (1994) [hep-th/9405187].
- [74] L. Kofman, A. D. Linde and A. A. Starobinsky, Phys. Rev. D **56**, 3258 (1997) [hep-ph/9704452].
- [75] K. Mukaida and K. Nakayama, JCAP **1408**, 062 (2014) [arXiv:1404.1880 [hep-ph]].
- [76] M. Bastero-Gil, R. Cerezo and J. G. Rosa, Phys. Rev. D **93**, no. 10, 103531 (2016) [arXiv:1501.05539 [hep-ph]].
- [77] R. N. Lerner and J. McDonald, Phys. Rev. D **80**, 123507 (2009) Phys-RevD.80.123507 [arXiv:0909.0520 [hep-ph]].
- [78] N. Okada and Q. Shafi, Phys. Rev. D **84**, 043533 (2011) [arXiv:1007.1672 [hep-ph]].

- [79] V. V. Khoze, *JHEP* **1311**, 215 (2013) [arXiv:1308.6338 [hep-ph]].
- [80] K. Nakayama and F. Takahashi, *JCAP* **1011**, 009 (2010) [arXiv:1008.2956 [hep-ph]].
- [81] R. Daido, F. Takahashi and W. Yin, arXiv:1702.03284 [hep-ph].
- [82] H. Y. Chen, I. Gogoladze, S. Hu, T. Li and L. Wu, arXiv:1703.07542 [hep-ph].
- [83] K. Greisen, *Phys. Rev. Lett.* **16**, 748 (1966).
- [84] G. T. Zatsepin and V. A. Kuzmin, *JETP Lett.* **4**, 78 (1966) [*Pisma Zh. Eksp. Teor. Fiz.* **4**, 114 (1966)].
- [85] V. S. Berezinsky and G. T. Zatsepin, *Phys. Lett.* **28B**, 423 (1969).
- [86] K. Murase and E. Waxman, *Phys. Rev. D* **94**, no. 10, 103006 (2016) [arXiv:1607.01601 [astro-ph.HE]].
- [87] Meures. Thomas, “Development of a Sub-glacial Radio Telescope for the Detection of GZK Neutrinos,” Springer, 2015.
- [88] M. Ibe and K. Kaneta, *Phys. Rev. D* **90**, no. 5, 053011 (2014) [arXiv:1407.2848 [hep-ph]].
- [89] G. F. Giudice and R. Rattazzi, *Phys. Rept.* **322**, 419 (1999) [hep-ph/9801271].
- [90] A. de Gouvêa and A. Kobach, *Phys. Rev. D* **93**, no. 3, 033005 (2016) [arXiv:1511.00683 [hep-ph]].
- [91] R. Bousso, D. M. Katz and C. Zukowski, *Phys. Rev. D* **92**, no. 2, 025037 (2015) [arXiv:1504.00677 [hep-th]].
- [92] L. Pogosian and A. Vilenkin, *JCAP* **0701**, 025 (2007) [astro-ph/0611573].
- [93] L. Pogosian, A. Vilenkin and M. Tegmark, *JCAP* **0407**, 005 (2004) [astro-ph/0404497].
- [94] M. Tegmark, A. Vilenkin and L. Pogosian, *Phys. Rev. D* **71**, 103523 (2005) [astro-ph/0304536].